Titanium oxide film for the bottom antireflective layer in deep ultraviolet lithography

Byung-Hyuk Jun, Sang-Soo Han, Kyong-Sub Kim, Joon-Sung Lee, Zhong-Tao Jiang, Byeong-Soo Bae, Kwangsoo No, Dong-Wan Kim, Ho-Young Kang, and Young-Bum Koh

Titanium oxide thin film, fabricated with tetraisopropyltitanate and oxygen by electron cyclotron resonance–plasma-enhanced chemical vapor deposition, is investigated as a potential candidate for the antireflective layer in KrF excimer laser (248-nm) lithography. The oxygen flow-rate dependence of the optical properties such as the refractive index (n) and the extinction coefficient (k) of the film at the 248-nm wavelength has been characterized, and the films with the expected combinations of n and k values for the antireflective layer have been deposited. Simulation results indicate that reflectance values of less than 4% and as low as 1.2% can be reached at the interface between the photoresist and the film postulating the structures of the photoresist/300-Å TiO_x film/c-Si substrate and the W-Si substrate, respectively, by selected proper combinations of n and k values. Moreover the reflectance can be further reduced to almost zero by changing the film thickness. Thus it is found that titanium oxide thin films can be used as the bottom antireflective layer in KrF excimer laser lithography. © 1997 Optical Society of America

Key words: Bottom antirefractive layer, titanium oxide thin film, reflectance, KrF excimer laser lithography.

1. Introduction

In the semiconductor lithographic process, antireflective films not only permit better linewidth control but also permit the realization of designs that were previously impossible to print. New high-performance antireflective layers (ARL's) for lithography with the i-line (365 nm), the KrF (248 nm), and even the ArF (193 nm) excimer lasers have been developed for nearly a decade in the semiconductor industry.[1–4]

As the linewidths in semiconductor manufacturing decrease, the use of shorter-wavelength light in the projection tools is indispensable. For the 0.35-μm and 0.25-μm feature sizes, the wavelengths of 365 nm and 248 nm are to be used, respectively. However, the reflectivity at the interface between the photoresist (PR) and the substrate increases as the wavelength of the light decreases. For example, the reflectance increases from 24% at 436 nm to 53% at 248 nm for a Si substrate and from 31% to 35% for a W-Si substrate. The increase in the reflectivity at the interface between the PR and the substrate causes a critical dimension variation that is due to the multiple interference effects as well as the reflection from the substrate topography. Thus, the notching and swing effects are significantly enhanced in the lithographic process.

A simple analytical expression for the reflectivity swing ratio (S, R_{max}/R_{min}) that is due to thin-film interference is as follows[5]:

$$S = 4\sqrt{R_1 R_2}\exp(-\alpha D), \quad (1)$$

where R_1 is the reflectivity at the air–photoresist interface, R_2 is the reflectivity at the photoresist–substrate interface, and α and D are the absorption coefficient and the average thickness of the photoresist, respectively. A top antireflective layer (TARL)[6,7] and a bottom antireflective layer (BARL) can reduce R_1 and R_2, respectively. The schematic structures for the TARL and BARL are shown in Fig. 1. The use of the TARL significantly reduces the

D-W. Kim, H-Y. Kang, and Y-B. Koh are with the Semiconductor R/D Center, Samsung Electronics Company Ltd., Yongin-Si, Kyungki-Do, 449-900, Korea. The other authors are with the Department of Materials Science and Engineering, Korea Advanced Institute of Science and Technology, Kusung-Dong, Yusung-Gu, Taejon, 305-701, Korea.

Received 19 April 1996; revised manuscript received 18 July 1996.
0003-6935/97/071482-05$10.00/0
© 1997 Optical Society of America

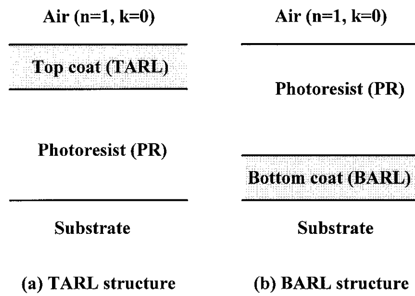

Fig. 1. Schematic structures for the (a) TARL and (b) BARL structures.

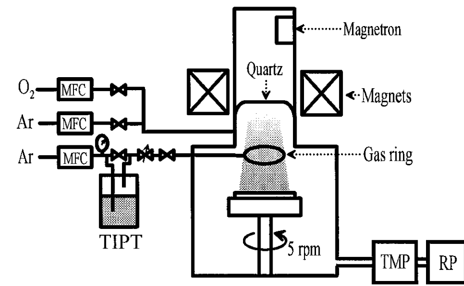

Fig. 2. Schematic diagram of the ECR–PECVD system used in the deposition of titanium oxide films: MFC, mass flow controller; TMP, turbomolecular pump; RP, rotary pump.

swing ratio by reducing R_1. Assuming a nonabsorbing film and normally incident radiation, R_1 is reduced to zero when $n_{\text{top coat}} = \sqrt{n_{\text{resist}}}$ (n is the refractive index) and the optical thickness of the coating is a quarter wavelength ($\lambda/4n_{\text{top coat}}$). The TARL can reduce only the swing effect without reducing the notching problem. In contrast, a BARL, which lies between the photoresist and substrate, can reduce the reflective notching by significantly reducing R_2. Under the same assumptions as the TARL, R_2 is reduced to zero when $n_{\text{bottom coat}} = \sqrt{n_{\text{resist}}\, n_{\text{substrate}}}$ and $d_{\text{bottom coat}} = \lambda/4n_{\text{bottom coat}}$. Thus a BARL could eliminate both the swing and notching problems in the lithographic process, so it is the most complete solution to obtaining a high resolution in deep-ultraviolet lithography.

Recently, amorphous carbon[1,8] and inorganic materials such as SiO_xN_y:H[2] and SiC[9] have been investigated as candidates for the BARL in deep-ultraviolet lithography. In this study, titanium oxide film was chosen as the BARL material in KrF excimer laser lithography, because it is expected that the optical constants (refractive index n and extinction coefficient k) of titanium oxide film at the wavelength of 248 nm are fitted to the optimum ARL condition that is discussed here.[10] In this study, the optical characterizations of titanium oxide films prepared by electron cyclotron resonance–plasma-enhanced chemical vapor deposition (ECR–PECVD)[11,12] are carried out. Moreover, an optical design simulation process is employed to find the optimum condition of zero reflectance between the PR and film and to calculate the reflectance in the fabricated films. Based on these results, the applicability of amorphous titanium oxide films as the BARL in KrF excimer laser lithography is discussed.

2. Experiment

The titanium oxide film was deposited in an ECR–PECVD system that could fabricate the dense and high-quality thin film without substrate heating and damage. The schematic diagram for the ECR–PECVD system used in the deposition of titanium oxide films is shown in Fig. 2. The titanium oxide films on (100) p-type Si substrates were deposited by using $Ti(O\text{-}i\text{-}C_3H_7)_4$ (tetraisopropyltitanate, or TIPT) and O_2 gas. TIPT is a suitable titanium precursor because it has an adequate vapor pressure even at room temperature.[13,14] O_2 gas (5 N) to form the ECR layer was introduced into the plasma chamber, and TIPT was introduced into the reaction chamber by means of a heated gas ring to protect condensation. The TIPT maintained to 65 °C was bubbled by Ar gas (5 N) at 10 sccm (where sccm denotes cubic centimeter per minute at STP), and a constant flow rate was achieved by controlling conductance with a metering valve. These excited oxygen and TIPT gases formed the titanium oxide film on the Si substrate located on a susceptor that could be rotated and moved up or down and heated up to maximum 700 °C by a resistant heater. The vacuum pump consisted of a turbomolecular pump and rotary pump. Pressures were measured in the reaction chamber and in the front of the rotary pump by an ionization gauge and a convectron gauge, respectively. Gases were introduced after evacuating the chamber and lines to the base pressure of 10^{-5} Torr, and the deposition was done at a pressure of 3×10^{-3} Torr. The deposition characteristics were controlled by various O_2 flow rates (5–30 sccm).

We performed a thin-film x-ray diffraction (Rikagu Inc., with a Cu target and Ni filter) analysis to investigate the crystallinity of the films under the conditions of tube voltage, 30 kV; tube current, 60 mA; incident beam angle, 3°; and scanning speed, 4°/min. The thickness, refractive index, and extinction coefficient at the 248-nm wavelength were evaluated by a spectroscopic ellipsometer (SOPRA SE ESVG). The reflectance at the interface between the photoresist and TiO_x (BARL) film under the structure of PR/300-Å TiO_x/Si or the W-Si substrate at the 248-nm wavelength with the matrix approach assuming a normal incident beam and a uniform and isotropic titanium oxide thin film has been calculated.

3. Results and Discussion

A. Deposition of Titanium Oxide Film

The titanium oxide films were deposited with a range of O_2 flow rates from 5 to 30 sccm at an ECR power of 300 W, a deposition temperature of room temperature, a TIPT bubbler temperature of 65 °C, and a working pressure of 3×10^{-3} Torr.

The x-ray diffraction analysis in Fig. 3 shows the films to be amorphous, which is important for optical homogeneity. All the films showed an almost con-

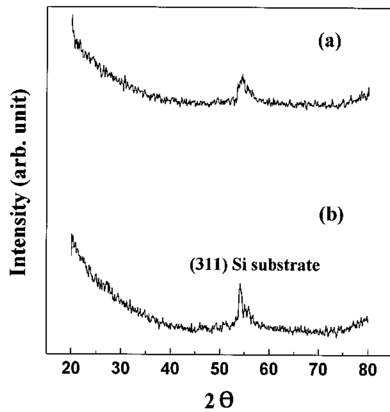

Fig. 3. X-ray diffraction analyses of TiO_x films deposited at 300 W at room temperature, with an O_2 flow rate of (a) 10 sccm, (b) 20 sccm.

stant deposition rate of approximately 30 Å/min, irrespective of the variation of O_2 flow rate.

Figure 4 shows the variation of the optical constants (n and k) of the films at the 248-nm wavelength as a function of O_2 flow rate in the range 5–30 sccm. The refractive index and extinction coefficient of the film, which are influenced by microstructure, compositional stoichiometry, and impurities in the film, vary from 2.09 to 2.32 and from 1.02 to 0.41, respectively, depending on the O_2 flow rate. The refractive index of the film deposited at the O_2 flow rate of 10 sccm shows a maximum value of 2.32, and as the O_2 flow rate increases to 30 sccm, it decreases because of the increase of oxygen incorporation in the film. The maximum point of the refractive index may be due to the mixing effects of plasma-forming efficiency variation by partial pressure variations of Ar and O_2 gases and optimum O_2 flow required to form the film. In contrast, the extinction coefficient decreases continuously as the O_2 flow rate increases from 5 to 30 sccm, and the film deposited at an O_2 flow rate of 5 sccm shows the highest extinction coefficient with the lowest refractive index.

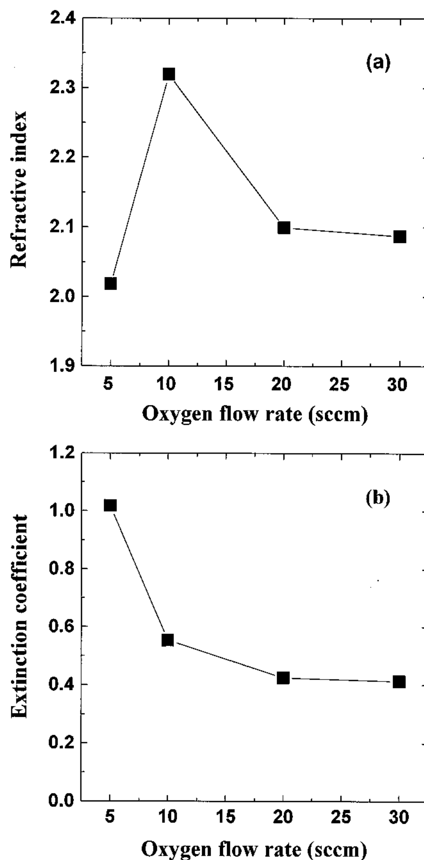

Fig. 4. Dependence of the TiO_x film optical constants on the O_2 flow rate at the 248-nm wavelength (deposition condition is 300 W, room temperature): (a) refractive index, (b) extinction coefficient.

B. Calculation of Reflectance

The reflectance (R) at the interface between the PR and ARL for the exposure wavelength of 248 nm could be calculated by using the following 2×2 characteristic matrix equation, assuming a normal incident beam on a uniform and isotropic thin film.[15]

$$R = \left| \frac{(n_{\mathrm{PR}} - ik_{\mathrm{PR}})B - C}{(n_{\mathrm{PR}} - ik_{\mathrm{PR}})B + C} \right|^2, \tag{2}$$

$$\begin{bmatrix} B \\ C \end{bmatrix} = \begin{bmatrix} \cos\delta & \dfrac{i \sin\delta}{n_f - ik_f} \\ i(n_f - ik_f)\sin\delta & \cos\delta \end{bmatrix} \begin{bmatrix} 1 \\ (n_{\mathrm{sub}} - ik_{\mathrm{sub}}) \end{bmatrix}, \tag{3}$$

where n_{PR} and k_{PR} are optical constants of the PR, and n_f and k_f are optical constants of the ARL, n_{sub} and k_{sub} are optical constants of the substrate, B is the standardized electrical field at the incident boundary plane, C is the standardized magnetic field at the incident boundary plane, and δ is the optical phase thickness equal to $[2\pi(n_f - ik_f)d/\lambda]$, where d is the physical film thickness and λ is 248 nm.

We considered the structures of the PR (× P89131; $n_{\mathrm{PR}} = 1.8$, $k_{\mathrm{PR}} = 0.011$ at 248 nm)/300-Å BARL/crystalline Si (c-Si) substrate ($n_{\mathrm{Si}} = 1.57$, $k_{\mathrm{Si}} = 3.565$ at 248 nm) or W-Si substrate ($n_{\mathrm{W\text{-}Si}} = 1.763$, $k_{\mathrm{W\text{-}Si}} = 2.546$ at 248 nm) for the calculation of the reflectance between the PR and ARL. The result of a three-dimensional simulated reflectance contour for the c-Si substrate is shown in Fig. 5(a). The reflectance goes to nearly zero at 248 nm when the ARL has approximately a refractive index of 2.11 and an extinction coefficient of 0.68, supposing a film thickness of 300 Å. Also, the result of the three-dimensional simulated reflectance contour for the W-Si substrate is presented in Fig. 5(b). The optimum condition of the ARL for the almost zero reflectance is when the refractive index and extinction coefficient are 2.05 and 0.59, respectively, at a film thickness of 300 Å. These simulation results are consistent with other simulation studies.[2,9] Thus, the optical constants of the titanium oxide films prepared in this study are nearly matched with the optimum condition for the antireflective coating in KrF excimer laser lithography.

The calculated reflectance at the interface between

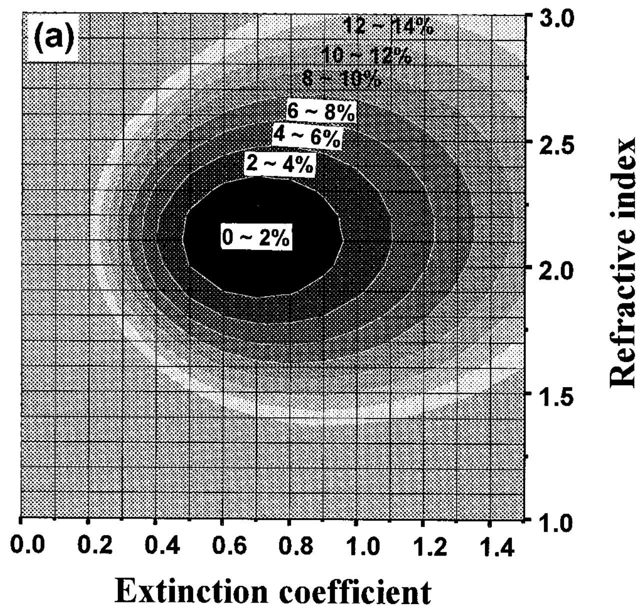

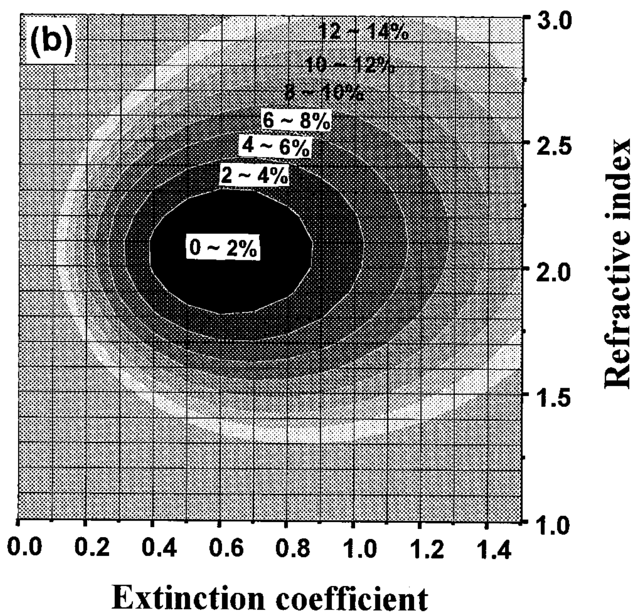

Fig. 5. Simulated reflectance contours at 248 nm: (a) PR(n_{PR} = 1.8, k_{PR} = 0.011)/300-Å ARL/*c*-Si (n_{Si} = 1.57, k_{Si} = 3.565); (b) PR(n_{PR} = 1.8, k_{PR} = 0.011)/300-Å ARL/W-Si ($n_{W\text{-}Si}$ = 1.763, $k_{W\text{-}Si}$ = 2.546).

the PR and the film for the structures of PR/300-Å TiO_x film/*c*-Si and PR/300-Å TiO_x film/W-Si, depending on the O_2 flow rate based on the optical parameters displayed in Fig. 4, is shown in Fig. 6. All the films in both structures exhibit a reflectance of less than 4%, which can be used as the antireflective coating in the practical lithographic process. Specifically, the reflectance can be reduced as low as 1.2% for the W-Si substrate when O_2 flow rate of 20 sccm is used.

The reflectance of the film can also be controlled by changing the film thickness. The simulated reflectance variations as a function of film thickness in both PR/TiO_x film/*c*-Si and PR/TiO_x film/W-Si structures, when it is supposed that optical constants are constant regardless of film thickness, are shown in Figs. 7(a) and 7(b), respectively. The reflectance of the film is strongly influenced by the film thickness. For the film thickness of less than 500 Å, which is preferred in the lithographic process, 0.9% reflectance of the film with the O_2 flow rate of 10 sccm is obtained at the film thickness of 250 Å for the Si substrate, and 0.1% reflectance of the film with the O_2 flow rate of 10 sccm is calculated at the film thickness of 225 Å for the W-Si substrate. Therefore the titanium oxide films prepared by ECR–PECVD can

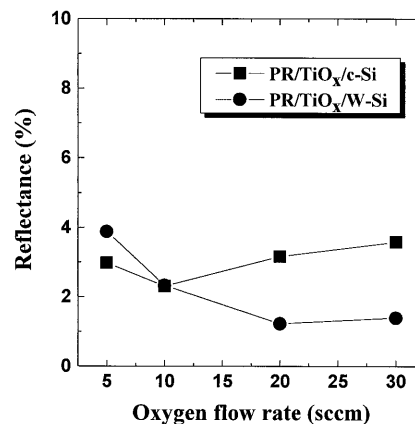

Fig. 6. Effect of O_2 flow rate on the reflectance at 248 nm for two structures of TiO_x films deposited at 300 W, room temperature (assuming a film thickness of 300 Å).

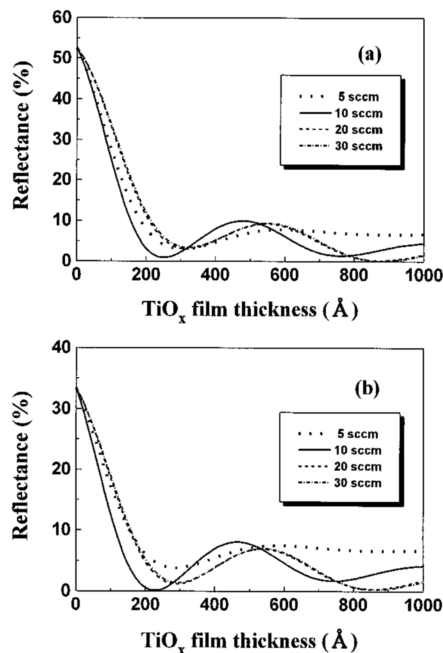

Fig. 7. Effect of the TiO_x film thickness on the reflectance at 248 nm with various O_2 flow rates (deposition condition is 300 W, room temperature): (a) PR/TiO_x/*c*-Si structure, (b) PR/TiO_x/W-Si structure.

be used as the antireflective layer in KrF excimer laser lithography by controlling the film thickness as well as the process parameters.

4. Conclusions

The uniform amorphous titanium oxide thin films were deposited by using an ECR–PECVD system at different O_2 flow rates for use as the antireflective layer in KrF excimer laser lithography. The refractive indices and the extinction coefficients of the films at the 248-nm wavelength lay in the range from 2.09 to 2.32 and from 1.02 to 0.41, respectively. Supposing a film thickness of 300 Å at the 248-nm wavelength, the optimum conditions for nearly zero reflectance are when there are an n_f of 2.11, k_f of 0.68 and an n_f of 2.05, k_f of 0.59 for Si and W-Si substrates, respectively. Thus these values are included in the range of optical constants of titanium oxide films with the selected O_2 flow rates. The calculated reflectance values at the interface between the PR and the film postulating the structures of PR/300-Å TiO_x film/*c*-Si and PR/300-Å TiO_x film/W-Si were less than 4% and as low as 1.2%, respectively. Also, the reflectance is very sensitive to the film thickness, so it could be reduced to almost zero by controlling the film thickness. Therefore, the titanium oxide films prepared by ECR–PECVD are optically applicable to the bottom antireflective layer in KrF excimer laser lithography.

B-H. Jun thanks C-K. Hwangbo of Inha University for valuable discussion.

References

1. Y. Suda, T. Motoyama, H. Harada, and M. Kanazawa, in "A new anti-reflective layer for deep UV lithography," in *Optical/Laser Microlithography V*, J. D. Cuthbert, ed., Proc. SPIE **1674,** 350 (1992).
2. T. Ogawa, M. Kimura, T. Gotyo, Y. Tomo, and T. Tsumori, in "Practical resolution enhancement effect by complete antireflective layer in KrF excimer laser lithography," in *Optical/Laser Microlithography VI*, J. D. Cuthbert, ed., Proc. SPIE **1927,** 263 (1993).
3. B. W. Dudley, S. K. Jones, C. R. Peters, D. A. Koester, G. A. Barnes, T. D. Flaim, and J. E. Lamb III, in "Enhancement of deep UV patterning integrity and process control using antireflective coating," in *Advances in Resist Technology and Processing IX*, A. E. Novembre, ed., Proc. SPIE **1672,** 638 (1992).
4. S. S. Miura, C. F. Lyons, and T. A. Brunner, in "Reduction of linewidth variation over reflective topography," in *Optical/Laser Microlithography V*, J. D. Cuthbert, ed., Proc. SPIE **1674,** 147 (1992).
5. T. A. Brunner, in "Optimization of optical properties of resist processes," in *Advances in Resist Technology and Processing VIII*, H. Ito, ed., Proc. SPIE **1466,** 297 (1991).
6. H. Yoshino, T. Ohfuji, and N. Aizaki, in "Process window analysis of the ARC and TAR systems for quarter micron optical lithography," in *Advances in Resist Technology and Processing XI*, O. Nalamasu, ed., Proc. SPIE **2195,** 236 (1994).
7. C. F. Lyons, R. K. Leidy, and G. B. Smith, in "Practicing the top antireflector process," in *Optical/Laser Microlithography V*, J. D. Cuthbert, ed. Proc. SPIE **1674,** 523 (1992).
8. Y. Tany, H. Mito, Y. Okuda, Y. Todokoro, T. Tatsuta, M. Sawai, and O. Tsuji, "Optimization of amorphous carbon-deposited antireflective layer for advanced lithography," Jpn. J. Appl. Phys. **32,** 5909–5913 (1993).
9. T. Ogawa, M. Kimura, Y. Tomo, and T. Tsumori, "Novel ARC optimization methodology for KrF excimer laser lithography at low K1 factor," in *Optical/Laser Microlithography V*, J. D. Cuthbert, ed., Proc. SPIE **1674,** 362 (1992).
10. E. D. Palik, ed., *Handbook of Optical Constants of Solids* (Academic, San Diego, Calif., 1985), Part II, Subpart 3, p. 795.
11. S. M. Rossnagel, J. J. Cuomo, and W. D. Westwood, *Handbook of Plasma Processing Technology* (Noyes, Park Ridge, N. J., 1990), Chap. 11, p. 285.
12. K. K. Schuegraf, *Handbook of Thin-Film Deposition Processess and Techniques* (Noyes, Park Ridge, N. J., 1988), Chap. 5, p. 147.
13. H. J. Frenck, W. Kulisch, M. Kuhr, and R. Kassing, "Deposition of TiO_2 thin films by plasma-enhanced decomposition of tetraisopropyltitanate," Thin Solid Films **201,** 327–335 (1991).
14. J. P. Lu, J. Wang, and R. Raj, "Solution precursor chemical vapor deposition of titanium oxide thin films," Thin Solid Films **204,** L13–L17 (1991).
15. H. A. Macleod, *Thin-Film Optical Filters*, 2nd ed. (Macmillan, New York, 1986), Chap. 2, p. 11.